Chapter 3
Cognitive Supervision for Transoral Laser Microsurgery

The thermal laser-tissue interactions described in Chap. 2 constitute the basic building block of laser microsurgery. In particular, ablation by vaporization is the process by means of which laser incisions and resections are performed. As we shall see in this chapter, these interactions need to be carefully monitored to ensure the formation of incisions as planned by the surgeon. Control of the laser effects on tissue is essential for the purpose of ensuring a safe and efficient surgical performance, which encompasses both resection accuracy and limited thermal damage to underlying and surrounding tissues.

Despite its importance, the control of the laser effects on tissues during Transoral Laser Microsurgery (TLM) is still performed manually, since available technologies do not include any support to monitor the state of tissues under laser irradiation. When analyzing the workflow of these interventions, it becomes apparent that the quality of laser resections depends entirely on clinicians, who must possess the experience required to anticipate and understand the results of their laser actions.

This chapter introduces the problem of the automatic supervision of laser-induced effects during laser surgery. A top-down approach is used to tackle this problem: specific circumstances in which surgeons would value enhanced information regarding the effects of their laser actions on tissues are identified. The problem is grounded in the identification of variables of interest that are selected as target for the supervision. In the scope of this thesis, we explore the application of artificial cognitive approaches to monitor these variables in a surgical scenario.

The first two sections of this chapter describe the current workflow of TLM and discuss its limitations from a clinical perspective. Our analysis is based both on evidence reported in medical literature, as well as on the opinions of clinicians who were consulted in the course of this doctoral research. In Sect. 3.3, we formulate the concept of a system capable of assisting clinicians during TLM, enhancing their perception of laser-induced effects on tissues. Two specific effects: thermal (temperature of tissues) and mechanical (laser cutting depth). We will review existing approaches to monitor these effects during laser irradiation, focusing on considerations regarding their

L. Fichera, *Cognitive Supervision for Robot-Assisted Minimally Invasive Laser Surgery*, Springer Theses, DOI 10.1007/978-3-319-30330-7_3

applicability in a TLM setup. To overcome the limitations of existing approaches, we will focus our attention on alternatives based on artificial cognitive methods. Section 3.4 describes our approach, which consists in the application of statistical learning to create models capable of predicting the aforementioned laser effects on tissues. This will lead us to the formulation of the research questions (in Sect. 3.5) that constitute the core of this doctoral dissertation, and that will be addressed in Chaps. 4 and 5. Finally, Sect. 3.6 presents the materials and methods used in our investigation.

3.1 Workflow of Transoral Laser Microsurgery

The typical surgical setup for TLM is represented in Fig. 3.1. The patient is positioned supine on the surgical bed and administered general anesthesia. A laryngoscope is inserted into his oral cavity down to the larynx: this tool consists of a rigid hollow shaft which provides a direct line-of-sight view of the surgical site. Because of the narrow size of the laryngeal lumen, these operations necessitate the use of a microscope: the average width of the larynx is well below 5.0 cm both in adult males and females [1].

The procedure begins with a visual preoperative inspection, aimed to (i) determine the location and extent of the lesion to be excised, and (ii) plan the intervention accordingly. In the example shown in Fig. 3.2a an inspection of the vocal folds is carried out, which reveals the presence of a superficial glottic tumor. To perform a closer analysis of the lesion, the surgeon might alternatively use a camera-equipped endoscopic device, which is delivered through the laryngoscope in proximity of

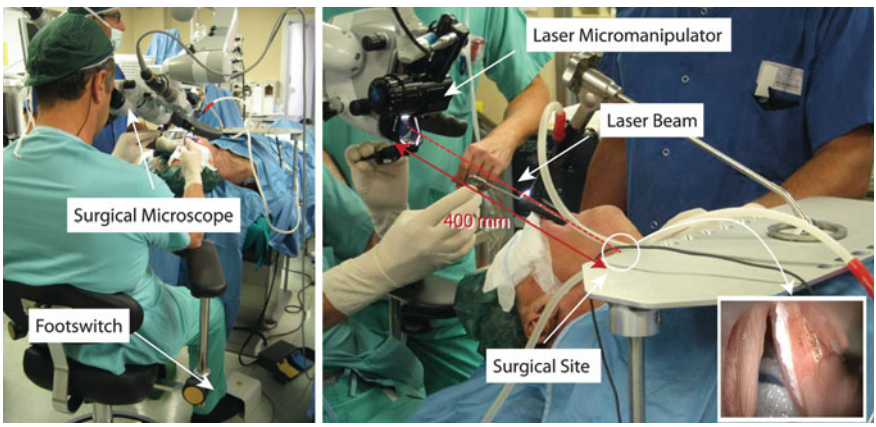

Fig. 3.1 Surgical setup for transoral laser microsurgery. Because of the minuscule size of the operating field, the intervention necessitates the use of a microscope. The laser activation is controlled by the surgeon through a footswitch. In the enlargement on the right, the laser micromanipulator is shown, which allows the surgeon to control the position of the surgical area. Distance between the micromanipulator and the surgical field is 400 mm (normal operating distance). Adapted from [2]

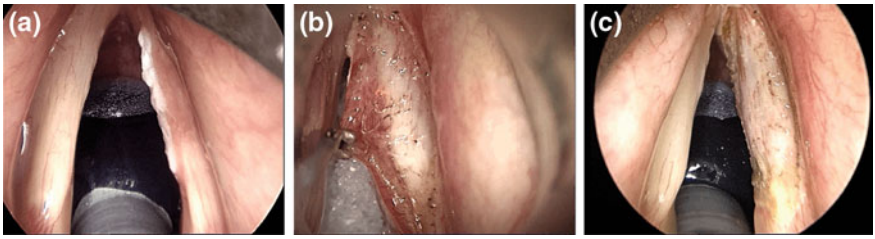

Fig. 3.2 Surgical excision of glottic squamous cell carcinoma. Here the surgical site is visualized through a microscope. The tumor is inspected during a preoperative examination (**a**) it appears as an irregular *white* mass on the surface of the right vocal fold. Tumor resection is shown in (**b**). Forceps are used to apply traction on the tissue, thus exposing the desired resection plane. The final result is shown in (**c**). Images courtesy of Prof. Giorgio Peretti, MD, Clinica Otorinolaringoiatrica, University of Genova

the lesion. During the inspection, the surgeon builds a plan of the procedure to be performed, which entails the selection of an appropriate resection technique and a preliminary mental plan of the dissection.

After the extent of resection has been determined, the tumor is excised with the laser. The carbon dioxide (CO_2) laser (wavelength 10.6 μm) is commonly used in TLM interventions, because of its optimal absorption properties in soft tissues of the larynx [3, 4]. The use of potassium titanyl phosphate (KTP) solid-state lasers (wavelength 532 nm) is also reported in the literature; other types of lasers (thulium, gold) are currently being evaluated [3].

In most surgical equipment, incisions are controlled manually moving the laser beam by means of a mechanical joystick and activating it through a footswitch (see Fig. 3.1) [3]. Forceps are used to apply traction on the tissue, exposing the desired resection plane (as shown in Fig. 3.2b). State-of-the-art laser systems incorporate robotic technology to offer the automatic execution of pre-programmed laser scan patterns. This concept is illustrated in Fig. 3.3: the coordination of one (or more) motorized reflective elements allows to realize diverse scan patterns. Tissue incision by laser scanning has been shown to be superior in terms of quality and accuracy with respect to manual control: laser scanning prevents the accumulation of heat by multi-pass irradiation, thus reducing the risk of thermal damage [6]. Nonetheless, the scanning mirrors commercially available still retain a manual element, i.e. they rely on the use of the traditional joystick to position the scan pattern on the desired incision line [2].

Small, well-delimited tumors are resected en bloc, as it is the case shown in Fig. 3.2b. A different technique is used for larger tumors: these are transected and removed in pieces [4]. It is important to point out that the primary objective of tumor resection is its complete eradication. This is known as *surgical radicality* and is a time-honored principle of surgery, based on the fact that an incomplete resection results in a recurrence of the disease [4]. To achieve sufficient radicality, the tumor is resected with an additional layer of healthy tissue that abuts it. The extent of this layer is decided by the surgeon based on the indications provided by the medical

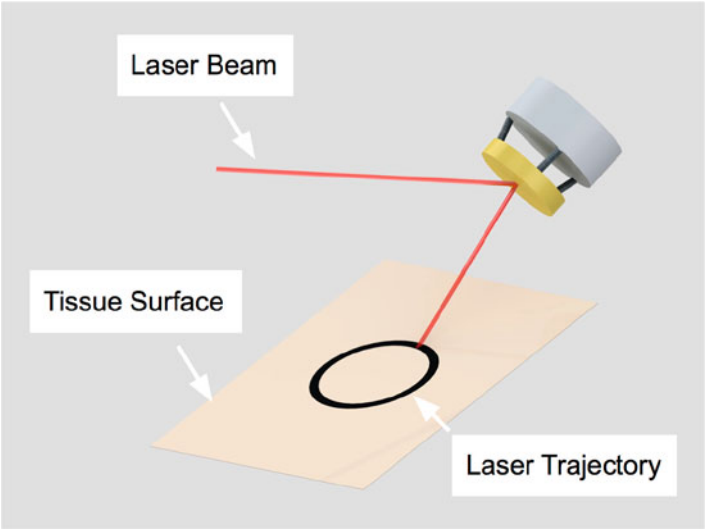

Fig. 3.3 Robotic laser micromanipulation system. The beam is deflected on the target by a 2-DOF steering mirror, which can be controlled to produce automatic laser trajectories. Adapted from [5]

literature: a typical resection margin for Squamous Cell Carcinoma (SCC) of the larynx is at least 5 mm [7, 8]. Once the tumor has been removed, an histological analysis is carried out to verify the appropriateness of the selected resection margins. The outcome of this examination is used to assess the possibility that residual cancer might have been left in situ. If the analysis reports any evidence of cancer in the margins, the physician might decide to repeat the surgical intervention.

Although TLM is primarily concerned with surgical radicality, in practice clinicians attempt to limit the size of the resection margins, in order to preserve as much healthy tissue as possible. This strategy is determined by the application of a second important medical principle, called *function preservation* [4], whose objective is to preserve the functionality of the organs being operated. In order to enable function preservation, the largest possible amount of healthy tissue that is not affected by the tumor should be spared. An example is shown in Fig. 3.2c: the SCC initially diagnosed on the right vocal fold (see Fig. 3.2a) has been resected without compromising the anatomical structure of the vocal fold, thereby allowing the patient to speak normally again after the intervention. Early stage tumors as the one shown in this example are particularly amenable to the application of function preservation strategies, however these may not be applicable in every case. Obtaining cancer-free (clear) margins remains of paramount importance to the aim of the procedure: incremental layers of tissue are removed until an appropriate margin is found [4].

In general, attaining resection margins that fulfill the requirements of both surgical radicality and organ preservation necessitates a correct surgical technique. As we shall see in the next section, this is particularly demanding in TLM.

3.2 Technical Limitations of Transoral Laser Microsurgery

Evidence of clear margins is required for a successful tumor resection, however the margins may be compromised by an inadequate laser cutting technique: lasers induce thermal artifacts on tissue, in the areas that surround the beam incidence point. These effects may be desirable to some extent—for instance, coagulation allows to avoid significant blood losses. Nonetheless, the creation of vast thermal damage might hinder the physician's interpretation of the adequacy of the resection margins both during the operation and the successive histological analysis, undermining any possible assessment of surgical radicality [9]. In this respect, another potential limiting factor is the usage of older surgical laser sources: the evolution of laser technology has led to the construction of ultra-pulsed CO_2 lasers which present narrower bands of thermal damage [6].

When function preservation is the aim, incision accuracy also becomes of fundamental importance. This is the case, for instance, of the resection of glottic tumours, in which reduced resection margins are selected for functional purposes. Typical values for these range between 1 and 2 mm, as larger values would result in a significant damage to the vocal function [7, 8]. To achieve such level of resection accuracy, both the width and depth of laser cuts need to be precisely controlled: to this aim, it is desirable to produce narrow incision widths, while the cutting depth should be as close as possible to the planned one. Even a few millimetres of additional resected tissue would greatly impact the functional outcomes of surgery [4].

The issues introduced above have been discussed with the clinicians involved in this research, during a series of interviews conducted in the initial stages of the μRALP project. From these interviews, it emerged that technologies currently in use for TLM do not include any functionality to support a correct laser cutting technique. As a result, nowadays the quality of resections relies entirely on the dexterity and experience of the clinician. Extensive training is required to develop an effective laser cutting. This includes the acquisition of a basic knowledge of the physical principles behind laser ablation of tissue, and the ability to manipulate the laser dosimetry parameters and its exposure time in order to obtain adequate cutting [3, 4]. Laser parameters used in clinical practice include power, energy delivery mode, pulse duration, incision scanning frequency and exposure time. At present times, no standard recipe exists to determine the parameters and the exposure required to obtain an optimal incision. Physicians use different settings, depending on their skills, experience and preferred technique [3].

Because of its contactless nature, laser surgery represents a challenge to clinicians: the lack of haptic feedback during laser cutting impairs the surgeon's perception of the incision depth and width. Furthermore, the thermal processes that occur during laser ablation are difficult to perceive, potentially leading to undesired tissue damage. Although experienced clinicians normally have sufficient knowledge and understanding of the laser ablation processes, the lack of perception of the effects of lasers on tissues represents a practical problem for many others.

In one of the interviews, we administered a questionnaire[1] aimed at understanding what new technological development clinicians would find most useful in the course of surgery. In their answers, clinicians indicated that technologies capable of monitoring the state of tissues during laser cutting would be useful to overcome the perception issues mentioned above; furthermore, they showed interest in the addition of novel safety functionalities to current laser systems: for instance, having an intelligent laser source that takes over the control of the intensity in selected dangerous circumstances, e.g. when the probability of thermal damage of tissues is high.

3.3 Supervision of the Laser Incision Process

From the evidence presented in the previous section, it emerges that clinicians do not have any technological support to monitor or control the quality of their laser incisions. Of particular interest are (i) thermal laser effects that could ultimately damage the tissues and (ii) the extent of laser resections. Here, we propose the creation of a *supervisory system*, in charge of monitoring these two important processes. The aim of such a system is to complement and enhance the surgeon's perception, providing information that would be difficult or impossible to obtain by visual inspection alone. We expect this will improve the surgeon's control of his laser actions, facilitating the creation of uniform and well-defined incisions, while minimizing thermal damage to surrounding tissues.

The concept of the supervisory system was originally formulated in [10]. The system is divided into two independent modules, each focusing on the monitoring of one of the processes mentioned above. In the following, we shall introduce these modules and discuss the challenges associated with their realization.

3.3.1 Monitoring of Tissue Overheating

This module monitors the temperature of tissues under direct laser irradiation and their surroundings. Figure 3.4 shows the type of supervision this technology may provide. For instance, the surgeon may be provided with an estimation of the temperature of tissues during laser cutting; or, with overheating alerts. Clinicians may use this information, e.g. stopping the cutting process if certain areas of tissue reach excessively high temperatures, and thus are likely to be get necrotic.

Traditional approaches to monitor the temperature of tissue during medical treatments require the placement of sensing equipment in direct contact with the measurement site [11]. These approaches are not applicable during TLM, due to space constraints: the surgical site is accessed through a transoral access which does not offer enough volume for the introduction of additional sensing equipment.

[1] available in Appendix A.

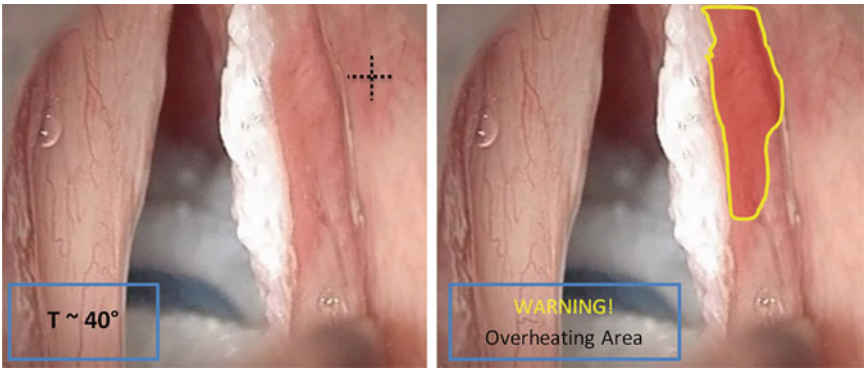

Fig. 3.4 Mock-up showing the on-line monitoring of tissue temperature. This module continuously estimates the superficial temperature of tissues on the surgical site. A cursor can be used to select a point-of-interest, whose temperature should be displayed (*left figure*). Alternatively, the temperature information can be used to issue safety alerts, e.g. if the probability of thermal damage of a zone exceeds a threshold level (*right figure*)

Non-invasive techniques based on common medical imaging technologies are currently being investigated [11]. These may require the introduction of substantial changes to the medical protocol, e.g. the use of MRI-compatible equipment. Furthermore, whether these methods account for the dynamic changes in temperature observed in a spatially concentrated area during laser microsurgery is to be verified.

The dynamics of tissue temperature describes how temperature spreads out in space during laser exposure as times goes on. As we have seen in the previous chapter, this phenomenon is described by the heat diffusion Eq. (2.12). Solutions to this inhomogeneous differential equation depend on the specific form of the input, as well as on the initial and the boundary conditions [12]. Solutions are commonly evaluated by means of numerical methods, as in [13–16]. These studies present models able to predict the temperature of tissue under specific conditions: laser wavelength, tissue type, temperature range. They coincide in saying that the variation of tissue temperature during laser irradiation is a complex phenomenon that involves non-linearities. These types of models are not straightforward to scale into an online predictive technology providing a temperature value of the tissue surface depending on the actions of the surgeon. Furthermore, a considerable number of parameters representing tissue and laser properties must be accounted for when modeling it. Accurate and real-time measurement of some of these parameters is not straightforward in a surgical setup. Laser motion during an incision includes an additional important challenge to the objective of modeling the thermal effects. To the best of our knowledge, none of the available models of temperature dynamics takes into account a scenario with a moving beam.

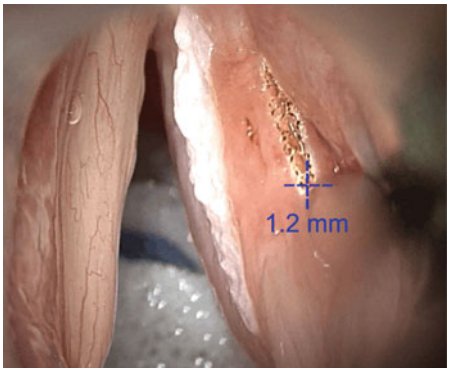

Fig. 3.5 Mock-up illustrating the concept of the online monitoring of the laser incision depth. This module continuously estimates the cutting depth reached by the laser

3.3.2 Monitoring of the Laser Incision Depth

This module monitors the incision depth as it develops during laser cutting. This information could be shown to clinicians (for example, as illustrated in Fig. 3.5), to enhance their perception of the laser cutting process.

Different approaches have been proposed to estimate the amount of tissue removed during laser ablation. However, none of them fulfill the necessary requirements to offer on-line estimation of incision depth. Methods based on mathematical modeling [17] and numerical simulations [18] have provided a viable solution to predict the ablation volume in hard tissue. These methods assume a specific tissue composition and their applicability to soft tissues is yet to be verified. Furthermore, these are computationally intensive and thus not suitable for on-line applications.

Alternative solutions, based on sensing, have been recently developed [19, 20]. Such solutions provide the capability of tracking the ablation crater during laser irradiation, without any *a priori* knowledge on the physical properties of tissue. However these approaches requires the use of additional sensing devices in the proximity of the ablation zone, limiting their applicability in TLM due to space constraints. The small size of the larynx does not offer enough volume for the introduction of additional equipment.

Recent advances in vision-based tissue surface reconstruction [21] seem a promising option to estimate the depth of laser ablation craters intraoperatively.

3.4 Cognitive Models

We propose to investigate the problem of monitoring the state of tissues during laser cutting using a virtual sensing approach [10]; i.e. we theorize that appropriate mathematical models can be used to map the application of laser energy to the resulting effects on tissue (incision depth and temperature variation). The input space

of these models coincide with the set of high-level laser inputs used by surgeons to control the laser incision process. The resulting effects on tissue depend on the combination of these parameters plus the total time of laser exposure.

These models are inspired and motivated by the capacity of humans beings to map and fuse diverse sets of information and infer the future state of events. Experienced surgeons possess the skills required to achieve precise and clean laser cutting, yet they certainly do not solve the complex differential equations that govern thermal laser-tissue interactions. This seems to indicate that they have a mental, probably not explicit, estimation about the state of the tissue, on the basis of which they tune the laser parameters and decide the amount of time the tissue should be exposed to the laser. Our intent is to create models that capture and reproduce this skill, mapping the high-level laser inputs to the resulting temperature of tissue and depth of laser incision. The problem of defining models capable of such behavior can be seen as the design of an artificial cognitive model [22].

Cognitive model generally denotes the combination of a knowledge set with a given cognitive architecture [23]. The knowledge captures the experience about a certain process or entity, while the cognitive architecture specifies how this knowledge is represented, acquired, and processed in order to implement some cognitive behavior. In the case of our models, we propose to acquire the necessary knowledge through supervised machine learning techniques.

Machine learning provides the means to approximate the behavior of a system or process without explicitly programming it: such behaviors are instead extracted from sample data. In the framework of statistical learning, knowledge about a process is represented in terms of a *hypothesis function* that describes its input/output characteristic [24]. *Learning* denotes the process of determining the form of the hypothesis function that better describes the process of interest. In a supervised learning setting, this search is performed on the basis of sample input/output pairs, collected during repeated observations of the process. In the next section, we shall formalize two hypothesis functions, aimed to describe laser effects (overheating and incision depth) on tissues during laser cutting. The remainder of the chapter will be dedicated to the materials and methods employed for the collection of the data sets required in the learning task.

3.5 Problem Formulation

Different parameters of the laser source can be manipulated to control the laser incision process. These include laser power (P) and scanning frequency (ω_s). In addition, the laser light can be delivered either as continuous wave or through intermittent pulses, with τ designating the duration of a single light pulse. Here, we model the influence of these parameters and that of the exposure time (t_{exp}) on (i) the superficial temperature of tissue and (ii) the laser incision depth. Our investigation starts out from two hypothesis functions, that are defined in the following subsections. Both hypotheses refer to a simple scenario, involving the laser incision of a slab of tissue.

For the sake of simplicity, we shall assume that the surface S of tissue is flat and smooth, i.e. it presents no irregularities, and that the laser beam is normally incident on it. Furthermore, we will assume that the laser beam is perfectly focused on the tissue surface, i.e. the radius of the laser spot on the surface of tissue equals the beam waist.

3.5.1 Temperature Hypothesis

To obtain an hypothesis that models the temperature dynamics of tissue, we start from a discretization of the surface of tissue into $n \times m$ squared superficial elements.

Definition 3.1 Let us define $\mathbf{T} \in \mathbb{R}^{n \times m}$ as the temperature of a set of $n \times m$ superficial elements.

Hypothesis 1 There exists a function, f, such that

$$\mathbf{T} = f(P, \tau, \omega_s, t_{exp}, \mathbf{T}_0) \tag{3.1}$$

Here, $\mathbf{T}_0$ is the temperature of tissue at the beginning of laser irradiation. Equation 3.1 estimates the temperature at any given point $p \in S$, given the laser parameters and inputs. Learning function f requires a dataset of L samples of the input/output variables $\left\{\mathbf{T}^i, (P, \tau, \omega_s, t_{exp}, \mathbf{T}_0)^i\right\}_{i=1}^{L}$. Based on these, Eq. 3.1 can be approximated using a supervised learning method.

3.5.2 Laser Incision Depth Hypothesis

We now formulate a similar hypothesis for the laser incision depth.

Definition 3.2 Let us define d as the incision depth produced by means of a laser in soft tissue; d identifies the altitude difference between the bottom of the laser crater and the surface of tissue.

Here, we further assume that the depth of incision created by means of laser scans is uniform across the incision width.

Hypothesis 2 There exists a function, f, such that

$$d = f(P, \tau, \omega_s, t_{exp}) \tag{3.2}$$

The model estimates the depth of laser incision based on the used laser parameters and inputs. To learn function f, a dataset $\left\{d^i, (P, \tau, \omega_s, t_{exp})^i\right\}_{i=1}^{L}$ is required.

3.6 Materials and Methods

The datasets required to learn the hypothesis functions (Eqs. 3.1 and 3.2) were collected through a series of controlled experiments. The experimental setup comprises a surgical laser source, which was used to study the effects of the laser parameters on the resulting incision depth and superficial temperature, and to derive the model intended to be used for estimation.

Laser motion and activation were controlled with a computerized system and the resulted incisions were examined under a microscope to measure their depth. Two forms of target: gelatin phantom tissue and ex-vivo chicken muscular tissue were used in the scope of this thesis. Measurement protocols were implemented to obtain the input-output pairs required to derive the forward model based on statistical regression techniques.

3.6.1 Controlled Incision of Soft Tissue

Incisions are produced by moving the laser beam along desired cutting paths on the tissue. Laser scanning, as described in [25], was used for this work: motorized mirrors are used to deflect the laser beam, enabling the automatic execution of pre-programmed cutting patterns. High-frequency cycles of the laser motion across the target tissue remove overlying layers with each pass.

The experimental setup (Fig. 3.6) uses a commercial surgical laser source, the Zeiss Opmilas CO2 25 (wavelength 10.6 μm, TEM_{00} beam profile), whose power is configurable in the range 2 to 25W. In the system used in this research, maximum power density is obtained when the laser spot is focused with a radius of 250 μm. Two energy delivery modes are provided, Continuous Wave (CW) and Repeated Pulse (RP), with the following pulse durations (τ): 0.05s, 0.1s, 0.2s, 0.5s. The concept of energy delivery mode will be further described in the next section. The CW/long-pulsed laser source used in this study has been superseded in clinical practice by short-pulsed (millisecond) lasers, which are known to produce more efficient cutting and reduced thermal damage [3]. However, the use of this equipment does not limit the applicability of the estimation methodology we propose. Our method, in fact, relies on a forward model mapping the laser inputs to the resulting effects on tissue. Thus, it can be applied to any laser source, provided that an appropriate forward model is used.

A motorized micromanipulator system previously developed in our laboratory [25] provides the controlled motion of the laser. This device regulates the motion of the laser through a tip/tilt fast steering mirror (S-334 manufactured by PI GmbH, Germany), with a maximum accuracy of 4 μm at a distance of 400 mm from the target (typical operating distance). The laser source and the micromanipulator are both connected to a Digital Operation Module (E-517 PI GmbH, Germany) which controls the motion and the activation of the laser. A user interface running on a GNU/Linux workstation allows the user to select exposure time, incision length and scanning speed.

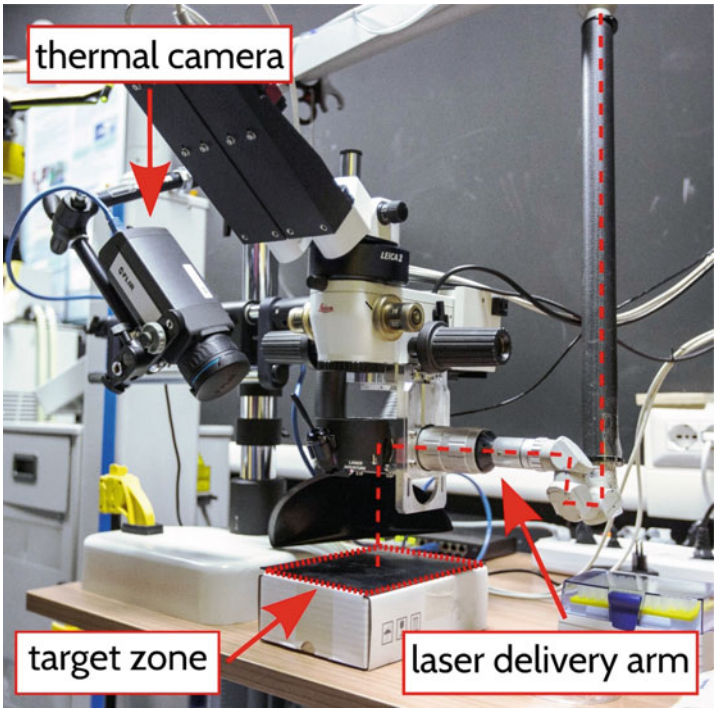

Fig. 3.6 Experimental setup. Tissue specimens are placed within the target zone. An infrared thermal camera (FLIR A655c) is used to monitor the temperature of tissue targets. The laser beam is delivered on the target through a passive articulated arm. A motorized micromanipulator provides the means to control the laser motion. Reproduced from [26] with kind permission from Springer Science+Business Media

3.6.2 Tissue Targets

Initial incision trials were conducted on tissue phantoms. Cylindrical agar-based gel targets were produced to mimic soft tissue. The constituents used to fabricate these targets are deionized water and agar powder (B&V s.r.l., Italy). The concentrations are as follows: 98 % water, 2 % agar. In soft tissues, the absorption of infrared laser radiation is dominated by the presence of free water molecules [12], therefore water was chosen as the main constituent of the targets. Although different from tissue, these gels offer a controlled medium on which the effects of the laser can be reproducibly studied [27].

In order to gather the data required for the learning tasks, additional incision trials were performed on fresh ex-vivo chicken muscle tissue. Like most soft tissues, chicken breast has a high water content, which makes it a convenient target for CO_2 laser ablation trials. Before the experiments, tissue samples were kept for 20 min in an open refrigerated box at a controlled temperature (7–12 °C), in order to preserve

their moisture and prevent degradation. To ensure identical initial temperature, the samples were monitored with an infrared thermal camera (Fig. 3.6). It is important to point out that the ex-vivo model selected in this study does not present the same laser absorption of in-vivo tissues. The thermal effects of a laser on living tissues is influenced by several factors that are not present in ex-vivo models [12], e.g. heat convection due to blood perfusion. Nonetheless, most of these factors can be neglected in first approximation [12]. The selection of an ex-vivo model is consistent with the objective of this study, i.e. to prove the concept of an on-line depth estimation system based on statistical regression analysis.

3.6.3 Measurement of Temperature During Laser Irradiation

Temperature of the surface of tissue is captured continuously during laser exposure plus a proportional time after the laser is turning off in order to capture the cooling down process. A digital thermal camera (FLIR A655, Flir Systems Inc., USA) equipped with a filter for CO_2 emissions. Data collected from the sensor is a stream of video frames with a resolution of 640×480 pixels at a rate of 100 Hz. A sample frame is shown in Fig. 3.7. The distance from the camera to the tissue was maintained constant throughout the experiments. At this distance, each pixel covers an area of $0.177 \times 0.177\,\text{mm}^2$.

3.6.4 Measurement of Depth of Incision

To examine the ablation craters, we used a digital microscope (Olympus SZX16). In order to get a complete exposure of the crater profile, tissue targets were sectioned into slices. Agar-based targets were sectioned manually with a blade. Ex-vivo soft

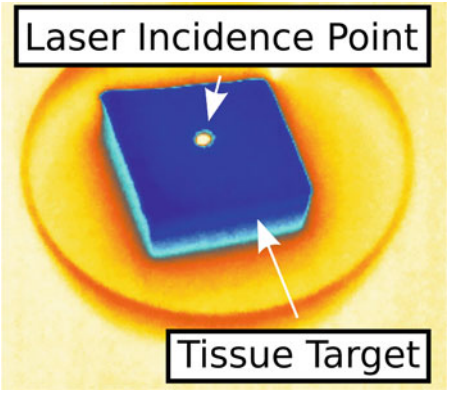

Fig. 3.7 Raw thermal image of phantom tissue target during laser irradiation. Brighter colors represent higher values of temperature. Reproduced from [26] with kind permission from Springer Science+Business Media

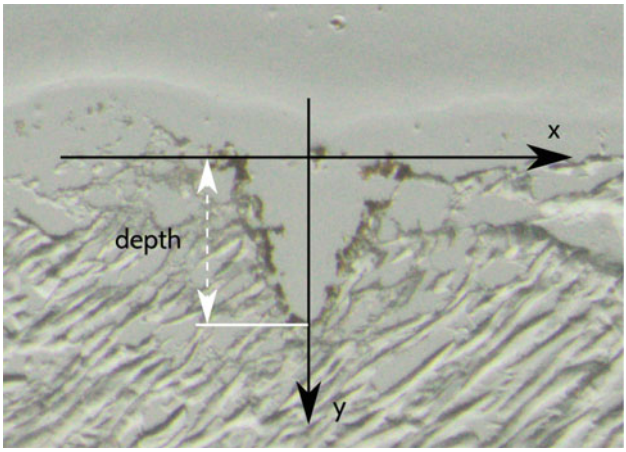

Fig. 3.8 Frozen section of chicken muscle tissue after laser ablation. The frame used for the measurement of the ablation depth is shown. Reproduced from [28] with kind permission from John Wiley & Sons, Ltd

tissue targets required a more articulated protocol, as manipulation and sectioning may induce deformation artifacts that alter the measurements process. To preserve the structural properties of these samples throughout the examination, a snap-freeze technique [29] was used. It consists in rapidly lowering the temperature of samples down to −70 °C, by means of dry ice. This technique increases the rigidity of specimens, allowing for sharp and clean slicing with minimum deformation. Targets were sectioned with a cryostat microtome, which allows to perform slicing while keeping the temperature of samples low (−30 °C). The depth of incision is defined as the distance from the surface to the bottom of the incision crater (see Fig. 3.8). This was measured through manual segmentation of the microscope images: the depth of incision is estimated contrasting its size in pixels against a reference scalebar.

References

1. M. Thiriet, in *Anatomy and Physiology of the Circulatory and Ventilatory Systems*, ser. Biomathematical and Biomechanical Modeling of the Circulatory and Ventilatory Systems (Springer, 2013)
2. L.S. Mattos, N. Deshpande, G. Barresi, L. Guastini, G. Peretti, A novel computerized surgeon-machine interface for robot-assisted laser phonomicrosurgery. Laryngoscope **124**(8), 1887–1894 (2014)
3. M. Rubinstein, W. Armstrong, Transoral laser microsurgery for laryngeal cancer: A primer and review of laser dosimetry. Lasers Med. Sci. **26**(1), 113–124 (2011)
4. W. Steiner, P. Ambrosch, in *Endoscopic Laser Surgery of the Upper Aerodigestive Tract: with Special Emphasis on Cancer Surgery* (Thieme, 2000)
5. D. Pardo, L. Fichera, D. Caldwell, L. Mattos, in "*Thermal Supervision During Robotic Laser Microsurgery*. 2014 5th IEEE RAS EMBS International Conference on Biomedical Robotics and Biomechatronics (2014), pp. 363–368
6. M. Remacle, G. Lawson, M.-C. Nollevaux, M. Delos, Current state of scanning micromanipulator applications with the carbon dioxide laser. Ann. Otol. Rhinol. Laryngol. **117**(4), 239–244 (2008)
7. M.L. Hinni, A. Ferlito, M.S. Brandwein-Gensler, R.P. Takes, C.E. Silver, W.H. Westra, R.R. Seethala, J.P. Rodrigo, J. Corry, C.R. Bradford, J.L. Hunt, P. Strojan, K.O. Devaney, D.R. Gnepp, D.M. Hartl, L.P. Kowalski, A. Rinaldo, L. Barnes, Surgical margins in head and neck cancer: A contemporary review. Head Neck **35**(9), 1362–1370 (2013)
8. M. Alicandri-Ciufelli, M. Bonali, A. Piccinini, L. Marra, A. Ghidini, E. Cunsolo, A. Maiorana, L. Presutti, P. Conte, Surgical margins in head and neck squamous cell carcinoma: what is close. Eur Arch. Oto-Rhino-Laryngol. **270**(10), 2603–2609 (2013)
9. G. Mannelli, G. Meccariello, A. Deganello, V. Maio, D. Massi, O. Gallo, Impact of low-thermal-injury devices on margin status in laryngeal cancer. An experimental ex vivo study. Oral Oncol. **50**(1), 32–39 (2014)
10. L. Fichera, D. Pardo, L.S. Mattos, in *Virtual Supervision for a Virtual Scalpel*. Proceedings of the 1st Russian-German Conference on Biomedical Engineering (Hanover, 2013)
11. P. Saccomandi, E. Schena, S. Silvestri, Techniques for temperature monitoring during laser-induced thermotherapy: An overview. Int. J. Hyperth. **29**(7), 609–619 (2013)
12. M. Niemz, *Laser-tissue Interactions* (Springer, Berlin, 2004)
13. J.J. Crochet, S.C. Gnyawali, Y. Chen, E.C. Lemley, L.V. Wang, W.R. Chen, Temperature distribution in selective laser-tissue interaction. J. Biomed. Opt. **11**(3), 034(031)–034(031–10) (2006)
14. S. Gnyawali, Y. Chen, F. Wu, K. Bartels, J. Wicksted, H. Liu, C. Sen, W. Chen, Temperature measurement on tissue surface during laser irradiation. Med. Biol. Eng. Comput. **46**(2), 159–168 (2008)
15. J. Jiao, Z. Guo, Thermal interaction of short-pulsed laser focused beams with skin tissues. Phys. Med. Biol. **54**(13), 4225 (2009)
16. E.M. Ahmed, F.J. Barrera, E.A. Early, M.L. Denton, C. Clark, D.K. Sardar, Maxwell's equations-based dynamic laser tissue interaction model. Comput. Biol. Med. **43**(12), 2278–2286 (2013)
17. S. Stopp, D. Svejdar, E. von Kienlin, H. Deppe, T.C. Lueth, A new approach for creating defined geometries by navigated laser ablation based on volumetric 3-d data. IEEE Trans. Biomed. Eng. 1872–1880 (2008)
18. L.A. Kahrs, J. Burgner, T. Klenzner, J. Raczkowsky, J. Schipper, H. Wörn, Planning and simulation of microsurgical laser bone ablation. Int. J. Comput. Assist. Radiol. Surg. **5**(2), 155–162 (2010)
19. B.Y. Leung, P.J. Webster, J.M. Fraser, V.X. Yang, Real-time guidance of thermal and ultrashort pulsed laser ablation in hard tissue using inline coherent imaging. Lasers Surg. Med. **44**(3), 249–256 (2012)

20. E. Bay, X.L. Deán-Ben, G.A. Pang, A. Douplik, D. Razansky, Real-time monitoring of incision profile during laser surgery using shock wave detection. J. Biophotonics (2013)
21. A. Schoob, D. Kundrat, L. Kleingrothe, L. Kahrs, N. Andreff, T. Ortmaier, Tissue surface information for intraoperative incision planning and focus adjustment in laser surgery. Int. J. Comput. Assist. Radiol. Surg. **10**(2), 171–181 (2015)
22. D. Vernon, Cognitive system. Encycl. Comput. Vis. (2012)
23. D. Vernon, G. Metta, G. Sandini, A survey of artificial cognitive systems: Implications for the autonomous development of mental capabilities in computational agents. IEEE Trans. Evol. Comput. **11**(2), 151–180 (2007)
24. M. Mohri, A. Rostamizadeh, A. Talwalkar, *Foundations of Machine Learning*, ser. Adaptive Computation and Machine Learning Series (MIT Press, 2012)
25. L. Mattos, G. Dagnino, G. Becattini, M. Dellepiane, D. Caldwell, "A virtual scalpel system for computer-assisted laser microsurgery," in Intelligent Robots and Systems (IROS). IEEE/RSJ Int. Conf. **2011**, 1359–1365 (2011)
26. D. Pardo, L. Fichera, D. Caldwell, L. Mattos, Learning temperature dynamics on agar-based phantom tissue surface during single point co2 laser exposure. Neural Process. Lett. **42**(1), 55–70 (2015). http://dx.doi.org/10.1007/s11063-014-9389-y
27. S. Rastegar, M.J.C. van Gemert, A.J. Welch, L.J. Hayes, Laser ablation of discs of agar gel. Phys. Med. Biol. **33**(1), 133 (1988)
28. L. Fichera, D. Pardo, P. Illiano, J. Ortiz, D.G. Caldwell, L.S. Mattos, Online estimation of laser incision depth for transoral microsurgery: approach and preliminary evaluation. Int. J. Med. Robot. Comput. Assist. Surg. (2015). http://dx.doi.org/10.1002/rcs.1656
29. M. Shabihkhani, G.M. Lucey, B. Wei, S. Mareninov, J.J. Lou, H.V. Vinters, E.J. Singer, T.F. Cloughesy, W.H. Yong, The procurement, storage, and quality assurance of frozen blood and tissue biospecimens in pathology, biorepository, and biobank settings. Clin. Biochem, **47**(4), 258–266 (2014)